ORIGIN OF NOTOCHORD

Development of the annelid axochord: Insights into notochord evolution

Antonella Lauri,[1*†] Thibaut Brunet,[1*] Mette Handberg-Thorsager,[1,2‡] Antje H.L. Fischer,[1§] Oleg Simakov,[1] Patrick R. H. Steinmetz,[1||] Raju Tomer,[1,2¶] Philipp J. Keller,[2] Detlev Arendt[1,3#]

The origin of chordates has been debated for more than a century, with one key issue being the emergence of the notochord. In vertebrates, the notochord develops by convergence and extension of the chordamesoderm, a population of midline cells of unique molecular identity. We identify a population of mesodermal cells in a developing invertebrate, the marine annelid *Platynereis dumerilii*, that converges and extends toward the midline and expresses a notochord-specific combination of genes. These cells differentiate into a longitudinal muscle, the axochord, that is positioned between central nervous system and axial blood vessel and secretes a strong collagenous extracellular matrix. Ancestral state reconstruction suggests that contractile mesodermal midline cells existed in bilaterian ancestors. We propose that these cells, via vacuolization and stiffening, gave rise to the chordate notochord.

Defining the properties and characteristics of the last common ancestor of bilaterian animals, Urbilateria, is a key question of the evolution and development field (*1*). In an attempt to infer a possible urbilaterian precursor for the chordate notochord (*2*, *3*), we reasoned that this structure should occupy a similar position with regard to overall morphology and molecular topography during development and in the adult body plan of living descendants (Fig. 1, A and B); that it should express, during its development, a suite of genes that have proven specific and indispensable for notochord formation in the chordates; and that it should be of widespread occurrence in bilaterian body plans (Fig. 1C). We focused our search on the model annelid *Platynereis dumerilii*, which is amenable to molecular studies and has retained more ancestral features than *Drosophila melanogaster* or *Caenorhabditis elegans* (*4*). By looking for cell populations that would resemble the vertebrate chordamesoderm (a population of mesodermal midline cells that converge medially to give rise to the notochord; red in Fig. 1A), we identified segmental pairs of mesodermal cells on the non–bone morphogenetic protein (BMP) body side (*5*) that stood out by early and continuous expression of *colA1*, encoding collagen type A (Fig. 2, A to D). SiMView light sheet microscopy (*6*) revealed that these cells moved underneath the neuroectoderm toward the midline until they contacted their bilateral counterpart (movie S1 and Fig. 2E). Subsequently, these cells narrowed and elongated without a net increase in cell surface (fig. S1), and additional adaxial mesodermal cells were observed to intercalate between the elongating pairs (Fig. 2E), reminiscent of the processes by which the chordamesoderm converges and extends (table S1) (*7*). Lineage tracking by targeted photoconversion of the fluorescent protein kikGR confirmed the origin of these cells from the mesodermal bands (fig. S2).

The unique location, large size, and specific arrangement of the *Platynereis* mesodermal midline cells allowed their unambiguous identification after whole-mount in situ hybridization (WMISH) and thus expression profiling by confocal imaging. To test a possible homology of these cells with the chordamesoderm, we chose a chordamesoderm-specific gene set according to the following criteria: (i) specificity—their combined expression uniquely defines the chordamesoderm; (ii) conservation—their chordamesoderm expression is conserved in at least three of four vertebrate species; and (iii) function—they have proven essential for chordamesoderm development or signaling. We thus investigated expression of seven transcription factors (*brachyury*, *foxA*, *foxD*, *twist*, *not*, *soxD*, and *soxE*), the signaling molecules *noggin* and *hedgehog* [*chordin* appears absent from annelid genomes (*8*)], and the guidance factors *netrin* and *slit* (table S2 for references). Transcripts for all but one [the *not* gene (*2*)] were detected (figs. S3 to S5) in accordance with previously reported *brachyury* expression (*9*), and their coexpression confirmed by double WMISH (Fig. 2, F to L). Although none of the genes were exclusively expressed in the annelid mesodermal midline, their combined coexpression was unique to these cells (implying that mesodermal midline in annelids and chordamesoderm in vertebrates are more similar to each other than to any other tissue). It is unlikely that the molecular similarity between annelid and vertebrate mesodermal midline is due to independent co-option of a conserved gene cassette, because this would require either that this cassette was active elsewhere in the body (which is not the case) or that multiple identical independent events of co-option occurred (which is unparsimonious). As in vertebrates, the mesodermal midline resembles the neuroectodermal midline, which expresses *foxD*, *foxA*, *netrin*, *slit*, and *noggin* (figs. S6 and S7) but not *brachyury* or *twist*. However, unlike in chicken (*10*), the annelid mesodermal and ectodermal midline populations are not directly related by lineage (fig. S2). Last, the *Platynereis* mesodermal midline is devoid of *paraxis*, which is exclusively expressed in laterally adjacent mesoderm (fig. S8), in line with its vertebrate ortholog demarcating paraxial mesoderm (*11*). In vertebrates, this segregation depends on canonical Wnt signaling, with β-catenin–positive cells preferentially adopting a paraxial fate and position (*12*). Consistently, we observed nuclear localization of β-catenin in the more-lateral mesoderm only, and β-catenin overactivation converted the mesodermal midline toward a more lateral fate and position (fig. S8).

We next compared the developmental fate of annelid and vertebrate mesodermal midline cells. Phalloidin staining and expression analysis of muscle markers (fig. S9) revealed that, after elongation, the *Platynereis* mesodermal midline cells differentiate into the previously described "medial ventral longitudinal muscle" (*13*) (Fig. 3A). Given the ropelike appearance and axial position of this muscle, we propose to call it "axochord." A muscular nature of a putative invertebrate counterpart of the chordate notochord is consistent with the observation that in the most basal chordate, amphioxus, the notochord is composed of specialized muscle cells (*14*) and expresses the same muscle markers (*15*). We further observed segmental sets of transverse muscles connecting to the axochord ("ventral oblique muscles") (*13*) (Fig. 3, A and B, and fig. S3). Scanning electron microscopy revealed that, in adult worms, the axochord is deeply embedded in the fibrous sheath of the ventral nerve cord (*16*) and remains connected to the transverse muscles (Fig. 3, C and D). Immunostainings confirmed its axial position between neuropil and blood vessel (fig. S12; similar to the notochord; Fig. 1, A and B). Axochord contractility was evident from live imaging (fig. S9, E to G, and movie S2) and occurred in alternation with the transverse muscles (movie S3). Electron micrographs confirmed the muscular nature of axochordal cells and revealed a tight physical connection to transverse muscles (Fig. 3, E to I). Laser ablation of the axochord impaired crawling (fig. S10 and movie S4) and confirmed anchoring of the transverse musculature. Additionally, we found that the

[1]Developmental Biology Unit, European Molecular Biology Laboratory (EMBL), D-69117 Heidelberg. [2]Janelia Farm Research Campus, 19700 Helix Drive, Ashburn, VA 20147, USA. [3]Centre for Organismal Studies, University of Heidelberg, Heidelberg, Germany.
*These authors contributed equally to this work. †Present address: Institute for Biological and Medical Imaging and Institute of Developmental Genetics, Helmholtz Zentrum München, Ingolstädter Landstrasse 1, D-85764 Neuherberg, Germany. ‡Present address: Max Planck Institute of Molecular Cell Biology and Genetics, Pfotenhauerstrasse 108, 01307 Dresden, Germany §Present address: Department for Molecular and Cell Biology, Harvard University, 16 Divinity Ave, Cambridge, MA 02138, USA. ||Present address: Department for Molecular Evolution and Development, University of Vienna, Althanstrasse 14, A-1090 Wien, Austria. ¶Present address: Howard Hughes Medical Institute, Stanford University, Stanford, CA 94305, USA. **#Corresponding author. E-mail: detlev.arendt@embl.de**

Platynereis transverse muscles share a specific molecular profile (*en+foxD*; fig. S11) with the vertebrate pioneer myocyctes flanking the notochord (*17*).

We next examined whether an axochord is also present in other annelids, lophotrochozoans, or protostomes (Fig. 1C). Phalloidin stainings had revealed ventral midline muscles in almost all annelid families (table S3), yet in some cases only pairs of ventral muscles had been reported (*18*, *19*). One such example is *Capitella teleta*, which belongs to the second big clade of annelids, the Sedentaria (beside Errantia, to which *Platynereis* belongs). We investigated development and molecular identity of ventral muscle fibers in *Capitella* (*18*) and found that (i), preceding metamorphosis, these converge and fuse into an axochord (Fig. 4, A to D, and fig. S13); (ii) the expression patterns of *foxA*, *noggin*, *brachyury*, *netrin* (Fig. 4, B and D, and fig. S13, B and C); *twist2* (*20*); and *hedgehog* (*21*) are consistent with coexpression in the axochord; and (iii) pairs of transverse muscles connect to the *Capitella* axochord (Fig. 4E) as in *Platynereis*. We also investigated the annelid *Owenia fusiformis* that belongs to the most basal annelid family (*22*) and likewise found an axochord connected to transverse muscle fibers (Fig. 4F). A similar arrangement also occurs in mollusk (*23*) and brachiopod larvae (*24*), and ventral midline muscles are observed in most lophotrochozoan phyla (table S3), suggesting that an axochord is ancestral for lophotrochozoa. The lophotrochozoan axochord is a genuinely paired structure, composed of left and right adjacent muscle strands that often bifurcate anteriorly and/or posteriorly, as also observed in chaetognaths (Fig. 4, G and H), a possible protostome outgroup (*25*, *26*) (Fig. 1C).

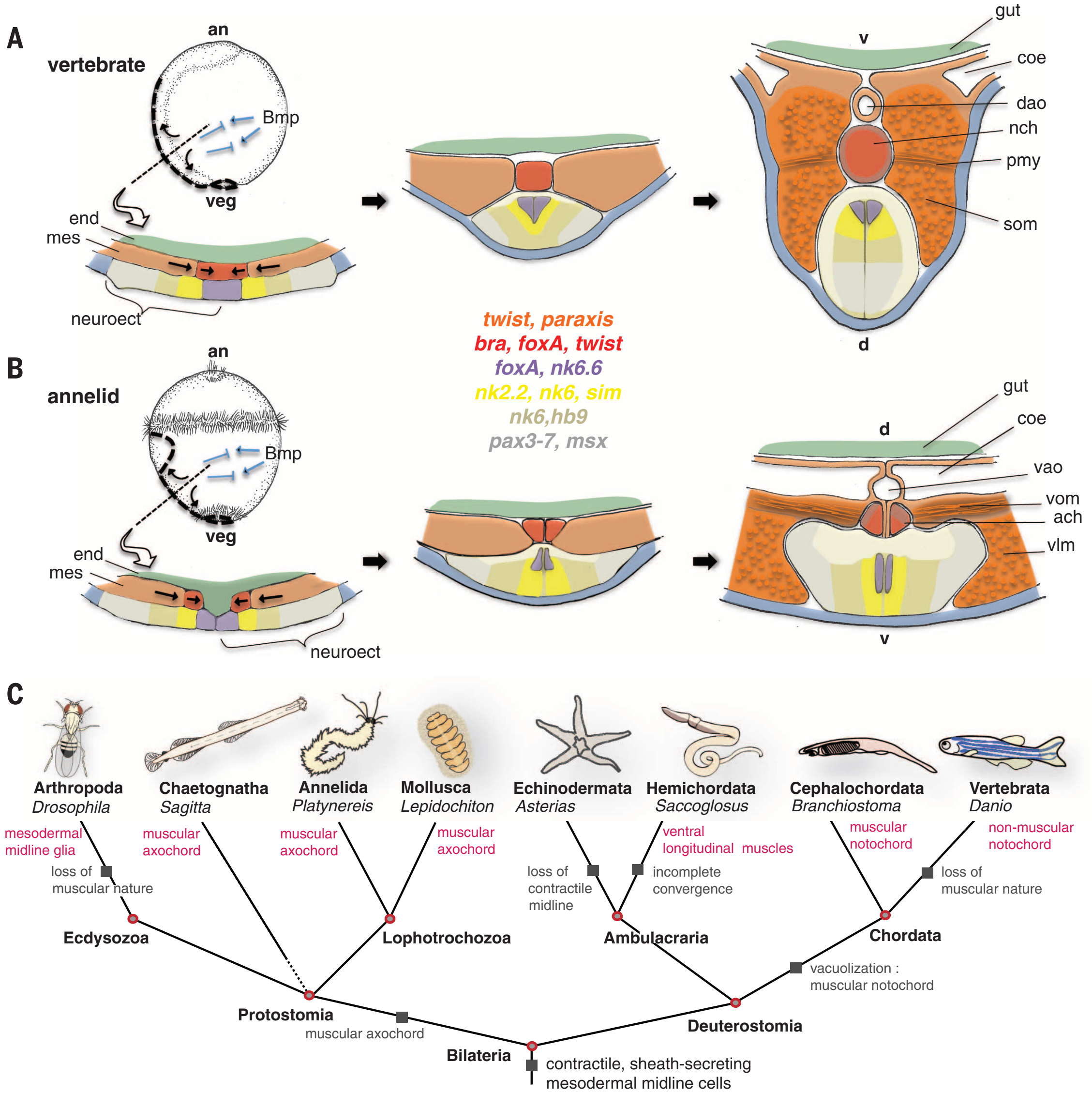

Fig. 1. Comparison of notochord and axochord development, gene expression, and anatomy. (**A**) Notochord development schematized for zebrafish at 9 hours post fertilization (hpf) or 90% epiboly, 14 hpf/neural keel, and 30 hpf/organogenesis stages. (**B**) Axochord development schematized for *Platynereis* at 34 hpf, 72 hpf, and 2 months of development. Top left images are in similar orientation with regard to the animal (an)–vegetal (veg) axis. Bold dashed lines represent lines of convergence of neuroectodermal and mesodermal cells, opposite to BMP signaling (blue arrows). The non-BMP body side will be dorsal (d) in vertebrate and ventral (v) in annelid, reflecting inversion of body posture in early chordate evolution (*35*). Thin black arrows indicate convergence and extension. Thin black dashed lines indicate positions of transverse sections (bottom left). Red, notochord (nch) or axochord (ach); orange, mesoderm (mes); purple, neuroectodermal midline; yellow, medial interneuron column; faint yellow, motor neuron column; gray, sensory interneuron column; blue, epidermis; green, endoderm (end)/gut. Transcription factors defining the respective tissues are written in corresponding colors. Bold black arrows indicate developmental progression. neuroect, neuroectoderm; coe, coelom; dao, dorsal aorta; pmy, primary myocyte; som, somite; vao, ventral aorta; vom, ventral oblique muscle; vlm, ventral longitudinal muscle. (**C**) Simplified phylogenetic tree. Black boxes illustrate the proposed evolutionary transition from ventral midline contractile cells to notochord.

An ancestral state reconstruction based on our data and on a survey of bilaterian musculature (table S3) favored the presence of an axochord in protostome ancestors (fig. S14).

Regarding deuterostomes, previous studies on the origin of the notochord focused on the hemichordate stomochord, an unpaired chordoid outpocketing of the pharynx, as a possible notochord homolog (*27*). Speaking against this hypothesis is its very anterior position and the absence of *brachyury*, *foxA*, and *noggin* expression (*27*, *28*). *goosecoid*, *hedgehog*, and *colA* expression rather suggest homology to the vertebrate prechordal plate (*29*–*33*). The pygochord, a stiff vacuolated rod in the posterior trunk of ptychoderid hemichordates (*34*), lies dorsal to the ventral blood vessel in the ventral mesentery. This stands in contrast to both axochord and

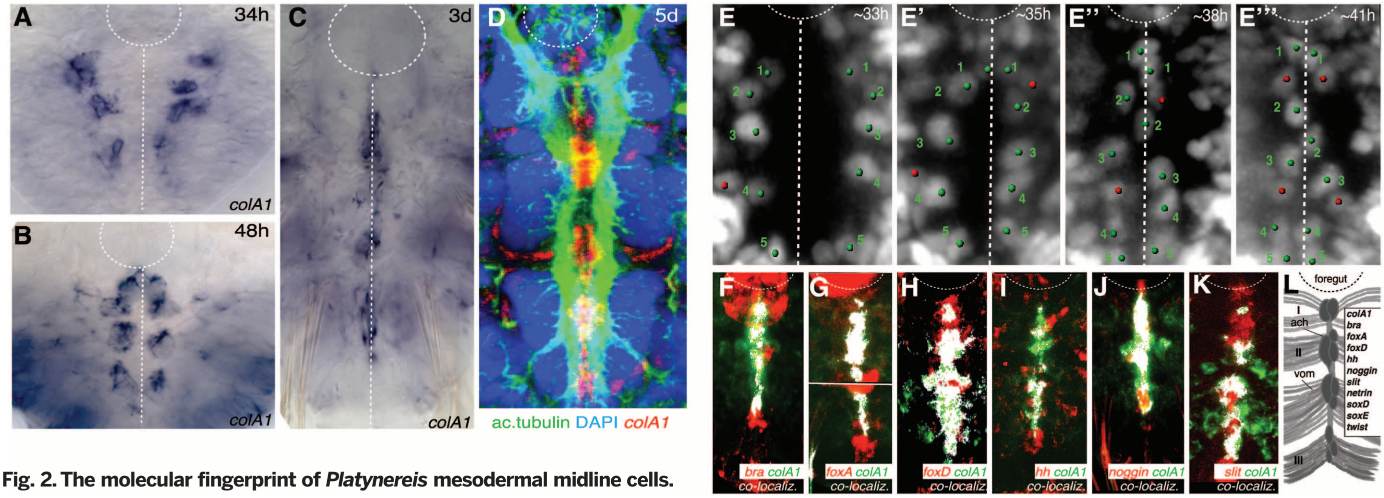

Fig. 2. The molecular fingerprint of *Platynereis* mesodermal midline cells. (**A** to **C**) Bright-field images and (**D**) confocal *z*-projection of *colA1* WMISH. Dotted white circle and line indicate foregut and midline, respectively. DAPI, 4′,6-diamidino-2-phenylindole. (**E** to **E'''**) Snapshots of SiMView time lapse of a live larva with fluorescently labeled nuclei showing ventrally converging (green dots) and intercalating (red dots) axochordal cells. Time interval, 2 to 3 hours. (**F** to **K**) Confocal *z*-projections of double WMISH 3-dpf larvae, ventral views, anterior up. (**L**) Explanatory scheme. vom also weakly express *colA* and *foxD*. Foregut also expresses *bra* and *foxA*.

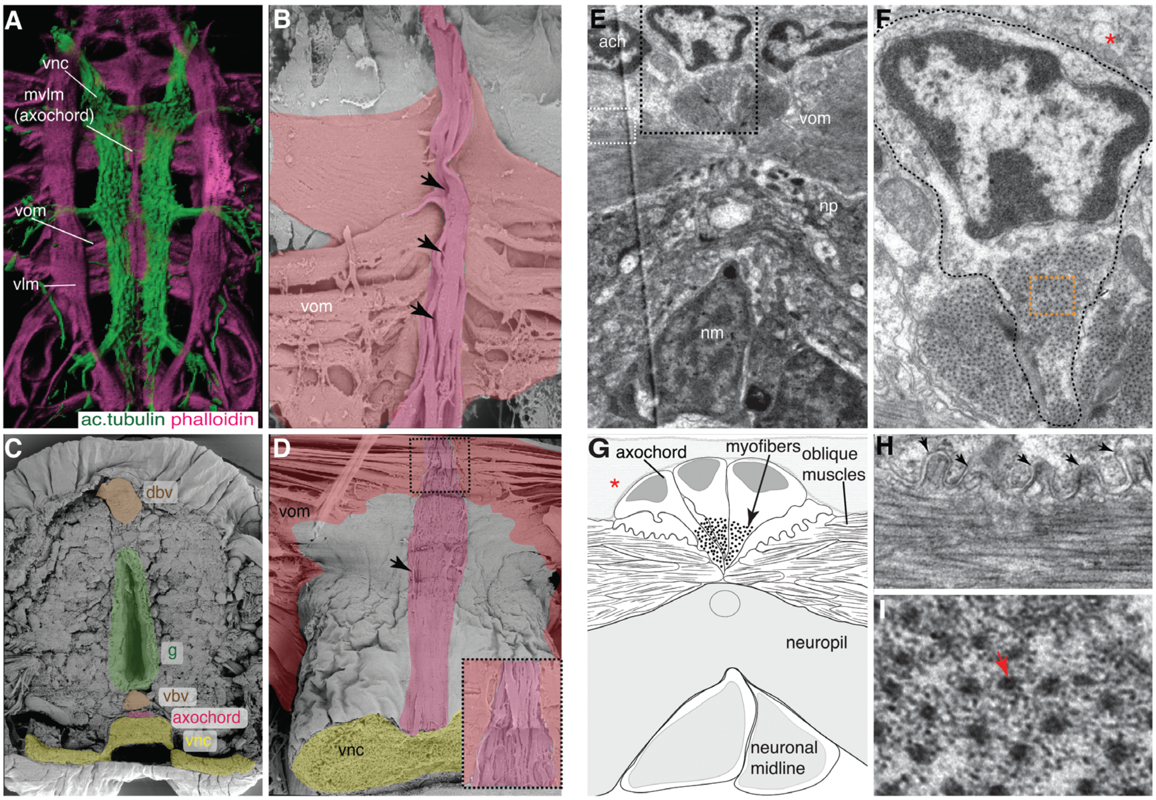

Fig. 3. The axochord is a ventral medial longitudinal muscle. (**A**) Ventral view of *Platynereis* immunolabeled musculature and nervous system, *z*-projection of confocal stack. Vnc, ventral nerve cord; mvlm, median ventral longitudinal muscle (axochord). (**B**) Pseudocolored scanning electron micrograph of *Platynereis* juvenile trunk, dorsal view. Axochord (deep pink) and attached oblique muscles (light pink). (**C** and **D**) Pseudocolored scanning electron micrographs. (C) Adult cross section. g, gut; vbv/dbv, ventral/dorsal blood vessel. (D) Dissected specimen showing axochord and oblique muscles embedded in the vnc sheath. Closeup illustrates axochord cell morphology. (**E**) Transmission electron micrograph showing axochordal cells, ventral oblique muscles, neuronal midline (nm), and the neuropil (np). (**F**) Closeup of area in black square in (E). One axochordal cell is outlined with dashed black line; asterisk indicates extracellular matrix. (**G**) Schematic drawing of (E). (**H**) Closeup of are in white square in (E), showing interdigitations between axochordal cells and oblique muscles. (**I**) Closeup of (F) (orange square) showing cross-sectioned myofibers (red arrow).

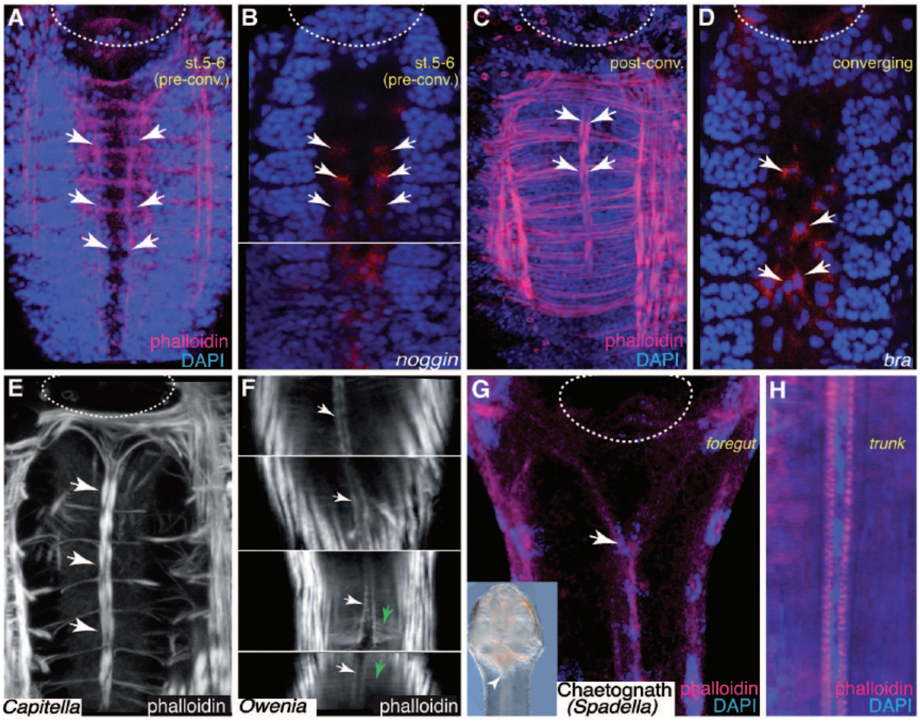

Fig. 4. An axochord is widespread in protostomes. (**A** to **D**) Convergence of ventral muscles into an axochord (white arrows) in *Capitella*, illustrated by phalloidin stainings (A and C) and WMISH (red in B and D) of selected axochord markers. (**E**) Axochord and transverse musculature in a stage-9 *Capitella* larva. Axochord bifurcation at the level of the foregut. (**F**) Axochord (white arrows) and transverse muscle fibers (green arrows) in juvenile *Owenia*, below the circumferential layer of longitudinal muscles. (**G**) Axochord (white arrow) in adult chaetognath (inset) bifurcating at the level of foregut. (**H**) Closeup of the axochord in the same specimen. Note elongated median nuclei and the two parallel strands of striated myofibers. All panels are *z*-projections of confocal stacks, ventral view, anterior up, white dashed line outlining foregut.

notochord, which are positioned between blood vessel and nerve cord (Fig. 1). Thus, vacuolization in the hemichordate stomochord and pygochord might have occurred independent to that of the chordate notochord. Unfortunately, no data are available for the specification and developmental fate of ventral mesodermal midline cells in hemichordates or larval echinoderms; except for *Protoglossus*, no ventromedian musculature has yet been observed (table S3).

Our study of annelid development reveals a population of mesodermal cells that converge and extend along the ventral midline and express a combination of transcription factors, signaling molecules, and guidance factors that closely matches that of the vertebrate chordamesoderm. These comparative data suggest that a similar population of mesodermal midline cells already existed in urbilaterian ancestors but leave open its ancient developmental fate. In annelids, these cells differentiate into an axochord; our investigation of chaetognath musculature and an ancestral state reconstruction based on comparative anatomy (fig. S14) suggest that a similar paired longitudinal muscle existed in protostome ancestors. Yet, in the absence of detailed investigations of expression profile and developmental fate of mesodermal midline cells in basal ecdysozoans and deuterostome ambulacrarians, the nature of ventral midline tissue in urbilaterians remains undecided. It might have constituted sheath-secreting mesenchyme that was independently converted into muscular axochord and notochord in lophotrochozoans and chordates, respectively; alternatively, this tissue might have been contractile already and transformed into axochord in protostomes and notochord in chordates (Fig. 1C). Regardless of its nature, dorsoventral axis inversion (*35*) would have brought the ventral midline tissue into a dorsal position in the chordate lineage, and the appearance of incompressible vacuoles (*14*) would have gradually transformed it into a stiff rod of constant length; the amphioxus notochord could then be regarded a vestige of a contractile-cartilaginous transition. This transition could have involved the co-option of *not* expression (which is absent from the axochord, see above) given that zebrafish *not* null mutants form muscle tissue instead of notochord (*36*). Last, in vertebrates, the notochord was complemented by a rigid backbone that crucially contributed to the success of our phylum.

REFERENCES AND NOTES

1. E. M. De Robertis, Y. Sasai, *Nature* **380**, 37–40 (1996).
2. D. L. Stemple, *Development* **132**, 2503–2512 (2005).
3. N. Satoh, K. Tagawa, H. Takahashi, *Evol. Dev.* **14**, 56–75 (2012).
4. A. S. Denes *et al*., *Cell* **129**, 277–288 (2007).
5. D. Arendt, K. Nübler-Jung, *Mech. Dev.* **61**, 7–21 (1997).
6. R. Tomer, K. Khairy, F. Amat, P. J. Keller, *Nat. Methods* **9**, 755–763 (2012).
7. J. B. Wallingford, S. E. Fraser, R. M. Harland, *Dev. Cell* **2**, 695–706 (2002).
8. O. Simakov *et al*., *Nature* **493**, 526–531 (2013).
9. D. Arendt, U. Technau, J. Wittbrodt, *Nature* **409**, 81–85 (2001).
10. M. Catala, M. A. Teillet, E. M. De Robertis, M. L. Le Douarin, *Development* **122**, 2599–2610 (1996).
11. R. Burgess, P. Cserjesi, K. L. Ligon, E. N. Olson, *Dev. Biol.* **168**, 296–306 (1995).
12. W. E. Reintsch, A. Habring-Mueller, R. W. Wang, A. Schohl, F. Fagotto, *J. Cell Biol.* **170**, 675–686 (2005).
13. A. H. Fischer, T. Henrich, D. Arendt, *Front. Zool.* **7**, 31 (2010).
14. J. E. Webb, *J. Zool.* **170**, 325–338 (1973).
15. M. M. Suzuki, N. Satoh, *Dev. Biol.* **224**, 168–177 (2000).
16. D. G. Baskin, *Tissue Cell* **3**, 579–587 (1971).
17. P. D. Currie, P. W. Ingham, *Nature* **382**, 452–455 (1996).
18. S. D. Hill, B. C. Boyer, *Biol. Bull.* **201**, 257–258 (2001).
19. A. Filippova, G. Purschke, A. B. Tzetlin, M. C. M. Müller, *Zoomorphology* **124**, 1–8 (2005).
20. K. K. Dill, K. Thamm, E. C. Seaver, *Dev. Genes Evol.* **217**, 435–447 (2007).
21. E. C. Seaver, L. M. Kaneshige, *Dev. Biol.* **289**, 179–194 (2006).
22. A. Weigert *et al*., *Mol. Biol. Evol.* **31**, 1391–1401 (2014).
23. M. Scherholz, E. Redl, T. Wollesen, C. Todt, A. Wanninger, *Curr. Biol.* **23**, 2130–2134 (2013).
24. A. Altenburger, A. Wanninger, *Front. Zool.* **6**, 3 (2009).
25. F. Marlétaz *et al*., *Curr. Biol.* **16**, R577–R578 (2006).
26. F. Marlétaz *et al*., *Genome Biol.* **9**, R94 (2008).
27. K. J. Peterson, R. A. Cameron, K. Tagawa, N. Satoh, E. H. Davidson, *Development* **126**, 85–95 (1999).
28. J. Gerhart, C. Lowe, M. Kirschner, *Curr. Opin. Genet. Dev.* **15**, 461–467 (2005).
29. J. Gerhart, *J. Cell. Physiol.* **209**, 677–685 (2006).
30. N. Miyamoto, H. Wada, *Nat. Commun.* **4**, 2713 (2013).
31. J. A. Belo, L. Leyns, G. Yamada, E. M. De Robertis, *Mech. Dev.* **72**, 15–25 (1998).
32. E. M. Pera, M. Kessel, *Development* **124**, 4153–4162 (1997).
33. A. W. L. Leung, S. Y. Y. Wong, D. Chan, P. P. L. Tam, K. S. E. Cheah, *Dev. Dyn.* **239**, 2319–2329 (2010).
34. K. Nübler-Jung, D. Arendt, *J. Zool. Syst. Evol. Res.* **37**, 93–100 (1999).
35. D. Arendt, K. Nübler-Jung, *Nature* **371**, 26 (1994).

ACKNOWLEDGMENTS

We thank A. Miyawaki for kikGR, R. Renkawitz-Pohl for the antibody against β-tubulin; P. McCrea for the antibody against β-catenin, A. Altenburger for brachiopod data; S. Kaul-Strehlow, G. Mayer, M. V. Sørensen, and K. Worsaae for insightful discussions; I. Haußer-Siller at the Electron Microscopy Core Facility (EMCF) (BioQuant, Heidelberg University); and the EMBL EMCF. The work was supported by the European Union's Seventh Framework Programme project "Evolution of gene regulatory networks in animal development (EVONET)" [215781-2] (A.L.), the Zoonet EU-Marie Curie early training network [005624] (A.F. and R.T.), the European Molecular Biology Laboratory (A.L., T.B., M.T.H., A.H.L.F., O.S.,P.R.H.S., and R.T.), the EMBL International Ph.D. Programme (A.L., T.B., A.H.L.F., P.R.H.S., R.T.), the Boehringer Ingelheim Foundation (O.S.), the Howard Hughes Medical Institute (P.J.K.), and the Visiting Scientist Program at the Janelia Farm Research Campus (M.H.T., R.T., D.A., and P.J.K.). A.L. and T.B. designed, performed, and documented most of the experiments; developed protocols; and wrote the manuscript. R.T. initiated and, together with M.H.T. and P.J.K., developed the *Platynereis* SiMView live imaging assay, and M.H.T. acquired the SiMView data. A.H.L.F. investigated musculature development and gene expression in *Platynereis*. M.H.T. contributed to the expression analysis. O.S. did transmission electron microscopy with T.B. and A.L. P.R.H.S. cloned and characterized *twist*. R.T. developed the injection protocol with N. Kegel and B. Backfisch. D.A. coordinated the study, wrote the manuscript, and drew the summary figure. The plasmid encoding the kikGR construct is covered by a material transfer agreement provided by the RIKEN Brain Science Institute. Alignments used for tree building are deposited on Dryad (10.5061/dryad.1ct82).

SUPPLEMENTARY MATERIALS

www.sciencemag.org/content/345/6202/1365/suppl/DC1
Materials and Methods
Figs. S1 to S16
Tables S1 to S3
References (*37–152*)
Movies S1 to S4

14 March 2014; accepted 6 August 2014
10.1126/science.1253396